Biomedical Optics EXPRESS

Rapid imaging of large tissues using high-resolution stage-scanning microscopy

Tao Yang,[1,2] Ting Zheng,[1,2] Zhenhua Shang,[1,2] Xiaojun Wang,[1,2] Xiaohua Lv,[1,2] Jing Yuan,[1,2] and Shaoqun Zeng[1,2,*]

[1]*Britton Chance Center for Biomedical Photonics, Huazhong University of Science and Technology-Wuhan National Laboratory for Optoelectronics, Wuhan 430074, China*

[2]*MoE Key Laboratory for Biomedical Photonics, Department of Biomedical Engineering, Huazhong University of Science and Technology, Wuhan 430074, China*

**sqzeng@mail.hust.edu.cn*

Abstract: Rapid and high-resolution imaging of large tissues is essential in biological research, like brain neuron connectivity research and cancer margins imaging. Here a novel stage-scanning confocal microscopy was developed for rapid imaging of large tissues. Line scanning methods and strip imaging strategy were used to increase the imaging speed. The scientific CMOS was used as line detector in sub-array mode and the optical sectioning ability can be easily adjusted by changing the number of line detectors according to different samples. Fluorescent beads imaging showed resolutions of 0.47 μm, 0.56 μm, and 1.56 μm in the X, Y, and Z directions, respectively, with a 40 × objective lens. A 10 × 10 mm^2 coronal plane with enough signal intensity could be imaged in about 88 sec at a sampling resolution of 0.16 μm/pixel. Rapid imaging of mouse brain slices demonstrated the applicability of this system in visualizing neuronal details at high frame rate.

OCIS codes: (180.0180) Microscopy; (180.1790) Confocal microscopy; (180.6900) Three-dimensional microscopy; (180.5810) Scanning microscopy; (170.3880) Medical and biological imaging.

References and links

1. M. Rajadhyaksha, R. R. Anderson, and R. H. Webb, "Video-rate confocal scanning laser microscope for imaging human tissues *in vivo*," Appl. Opt. **38**(10), 2105–2115 (1999).
2. J. Cushion, F. N. Reinholz, and B. A. Patterson, "General purpose control system for scanning laser ophthalmoscopes," Clin. Experiment. Ophthalmol. **31**(3), 241–245 (2003).
3. G. Q. Xiao, T. R. Corle, and G. S. Kino, "Real-time confocal scanning optical microscope," Appl. Phys. Lett. **53**(8), 716–718 (1988).
4. R. Wolleschensky, B. Zimmermann, and M. Kempe, "High-speed confocal fluorescence imaging with a novel line scanning microscope," J. Biomed. Opt. **11**(6), 064011 (2006).
5. C. J. R. Sheppard and X. Q. Mao, "Confocal microscopes with slit apertures," J. Mod. Opt. **25**, 1169 (1998).
6. K. B. Im, S. Han, H. Park, D. Kim, and B. M. Kim, "Simple high-speed confocal line-scanning microscope," Opt. Express **13**(13), 5151–5156 (2005).
7. A. L. Carlson, L. G. Coghlan, A. M. Gillenwater, and R. R. Richards-Kortum, "Dual-mode reflectance and fluorescence near-video-rate confocal microscope for architectural, morphological and molecular imaging of tissue," J. Microsc. **228**(1), 11–24 (2007).
8. Y. G. Patel, K. S. Nehal, I. Aranda, Y. Li, A. C. Halpern, and M. Rajadhyaksha, "Confocal reflectance mosaicing of basal cell carcinomas in Mohs surgical skin excisions," J. Biomed. Opt. **12**(3), 034027 (2007).
9. D. S. Gareau, Y. G. Patel, Y. Li, I. Aranda, A. C. Halpern, K. S. Nehal, and M. Rajadhyaksha, "Confocal mosaicing microscopy in skin excisions: a demonstration of rapid surgical pathology," J. Microsc. **233**(1), 149–159 (2009).
10. T. C. Schlichenmeyer, M. Wang, K. N. Elfer, and J. Q. Brown, "Video-rate structured illumination microscopy for high-throughput imaging of large tissue areas," Biomed. Opt. Express **5**(2), 366–377 (2014).
11. D. Xu, T. Jiang, A. Li, B. Hu, Z. Feng, H. Gong, S. Zeng, and Q. Luo, "Fast optical sectioning obtained by structured illumination microscopy using a digital mirror device," J. Biomed. Opt. **18**(6), 060503 (2013).
12. S. Abeytunge, Y. Li, B. Larson, R. Toledo-Crow, and M. Rajadhyaksha, "Rapid confocal imaging of large areas of excised tissue with strip mosaicing," J. Biomed. Opt. **16**(5), 050504 (2011).

#235822 - $15.00 USD Received 11 Mar 2015; revised 17 Apr 2015; accepted 17 Apr 2015; published 23 Apr 2015

13. M. A. Saldua, C. A. Olsovsky, E. S. Callaway, R. S. Chapkin, and K. C. Maitland, "Imaging inflammation in mouse colon using a rapid stage-scanning confocal fluorescence microscope," J. Biomed. Opt. **17**(1), 016006 (2012).
14. T. Zheng, Z. Yang, A. Li, X. Lv, Z. Zhou, X. Wang, X. Qi, S. Li, Q. Luo, H. Gong, and S. Zeng, "Visualization of brain circuits using two-photon fluorescence micro-optical sectioning tomography," Opt. Express **21**(8), 9839–9850 (2013).
15. H. Gong, S. Zeng, C. Yan, X. Lv, Z. Yang, T. Xu, Z. Feng, W. Ding, X. Qi, A. Li, J. Wu, and Q. Luo, "Continuously tracing brain-wide long-distance axonal projections in mice at a one-micron voxel resolution," Neuroimage **74**, 87–98 (2013).
16. J. B. Pawley and R. B. R. Masters, "Handbook of Biological Confocal Microscopy, Second Edition," OPTICE **35**, 2765–2766 (1996).
17. S. Deng, L. Liu, Z. Liu, Z. Shen, G. Li, and Y. He, "Line-scanning Raman imaging spectroscopy for detection of fingerprints," Appl. Opt. **51**(17), 3701–3706 (2012).
18. E. Dusch, T. Dorval, N. Vincent, M. Wachsmuth, and A. Genovesio, "Three-dimensional point spread function model for line-scanning confocal microscope with high-aperture objective," J. Microsc. **228**(2), 132–138 (2007).
19. T. Ragan, L. R. Kadiri, K. U. Venkataraju, K. Bahlmann, J. Sutin, J. Taranda, I. Arganda-Carreras, Y. Kim, H. S. Seung, and P. Osten, "Serial two-photon tomography for automated ex vivo mouse brain imaging," Nat. Methods **9**(3), 255–258 (2012).

1. Introduction

Rapid and high resolution imaging of large tissues can provide vital structure information and aid further study in a short period of time. In neuron science research, researchers want to study the structure of neurons for understanding the function of neuron circuit. Combined with fluorescence labelling technology, they can study the specified functional circuit. To acquire the entire neural structure, sub-micron resolution on a centimeter scale is needed for imaging system. Meanwhile, because of the individual difference and numbers of brain areas, lots of samples are needed to study in order to get statistical results. Therefore, there is an urgent need for the development of a high-speed imaging system with high-resolution.

The technique of stage-scanning microscopy has been proved very suitable for imaging large tissues. Generally, the approach for imaging large tissues by using stage-scanning confocal technique can be classified into two clusters, namely, mosaic imaging and strip imaging. In mosaic confocal microscopy, a mosaic image is obtained by scanning a focused beam within the field of view. In order to increase imaging speed, high-speed scanning devices (a polygon mirror [1], a resonant galvanometer [2]) and multiple beam scanning device (Nipkow disk [3]) are used. However, the imaging speed of these systems cannot be very fast because the sample is scanned point by point. The faster imaging speed can be achieved by using line scanning instead of point scanning. The mosaic images are scanned only in one direction such that the frame rate is significantly increased [4, 5]. One group have previously reported the development that they use line scanning method to achieve a high frame rate of 191 frames per sec for an image with 512 × 512 pixels [6]. However, mosaic confocal microscopy has the drawback of limited field of view. Especially when high numerical aperture objective was used to obtain high resolution and the field of view was reduced to less than 500 × 500 μm^2 [7]. It was indispensable to image numbers of mosaics in order to cover the entire specimen area [8–11]. Repetitive imaging is cost-ineffective since the stage will be controlled to go through an acceleration-constant speed-deceleration process, which is inefficient. This implies that non-imaging time is longer for larger tissues and can be considered to a waste of time. Furthermore, high-imaging uniformity is required to stitch all mosaic images together in order to obtain a full image.

Strip imaging methods combined with line illumination can significantly improve the overall imaging speed mainly by reducing non-imaging time. In strip imaging, the entire sample is divided into several strips and samples are imaged one strip at a time rather than the conventional mosaic imaging method. Recently, stage-scanning confocal microscopy combined with strip imaging was applied for rapid imaging of large specimens [12–15]. In these systems, line illumination is generated by scanning a focused beam on the sample. The signal is then detected point by point, which results in a slow or limited imaging speed. As a

#235822 - $15.00 USD Received 11 Mar 2015; revised 17 Apr 2015; accepted 17 Apr 2015; published 23 Apr 2015

result, in order to improve the scanning speed, the sampling resolution was reduced to about 1 μm/pixel.

In order to improve imaging speed at high sampling rate, a cylindrical lens is used to generate direct line illumination. The signal from a complete line could be simultaneously recorded using a linear detector. This afforded the advantage of avoiding off-axis aberrations, which occurred during specimen imaging by scanning the stationary laser beam across the specimens [16]. Line-illumination based on the stage-scanning has been used in many applications, like Raman imaging spectroscopy for detection of fingerprints [17]. However, in neural structure research, acquiring the detail structure of neuron over large area in a short time, for example, spines, boutons and axons, is challenging. It has created the need for the imaging system to have high resolution with high imaging speed. In this study, we developed a strip imaging confocal microscopy capable of imaging a large tissue (10×10 mm^2) at a high imaging speed (about 88 sec) with a high sampling resolution of 0.16 μm/pixel. The scientific CMOS was used as line detector to achieve high frame rate when it was working in the sub-array mode and the optical sectioning ability can be easily adjusted by changing the number of line detectors. Imaging with high sampling rate, we integrated signals from each line detector to acquire good image contrast.

2. Materials and methods

The configuration of the stage-scanning system used in this study is shown in Fig. 1(a). A 488-nm laser was used as the light source. The laser beam was expanded using two lenses (lens 1 and lens 2) in order to fill the aperture of the objective lens. The diffraction-limited illumination line was provided by an optical system, which included a cylindrical lens, a tube lens, and a high NA water objective lens (LUMPLFLN 40X water, NA 0.8, Olympus). Fluorescence emitted from the specimen was detected using a filter set. The specimen was fixed on a precision motion stage (X axis: ABL20020, Y axis: ANT130, Z axis: AVL125, Aerotech), possessing high repeatability (± 0.2 μm) and stability. The x-y plane of sample was scanned by moving the X and Y stage. And the z-axis scanning was implemented by moving the Z-stage. The sample was scanned during its movement across the static illumination line. The frame rate of the detector and the motion speed were synchronized to eliminate image blur. The motion speed was equated using the equation: $v = p / m \cdot f$, where 'p' is the pixel size of detector, 'm' is system magnification, and 'f' is the frame rate of the detector. Here, we used a scientific CMOS (ORCA-Flash 4.0, Hamamatsu Photonic K. K., Japan, 2048 × 2048 pixels) as line detector for sample imaging. The size of each pixel is 6.5μm × 6.5μm. This detector offered an extremely low readout noise, a large field of view along with a sub-array mode frame rate of 25656 frames/sec. According to the frame rate of sCMOS, the maximum motion speed was about 250 mm/min and it took about 2.4 sec to scan a 10 mm long strip. In order to use uniformity part of illumination line, the strip width was set to 330 μm and it cost about 0.5 sec to move laterally before imaging another strip. So a 10×10 mm^2 coronal plane could be imaged in $((2.4s + 0.5s) \times 10000 \div 330) - 0.5s \approx 88s$ at the sampling resolution of 0.16 μm/pixel.

The scheme of imaging is shown in Fig. 1(b). sCMOS was controlled to capture images at every time point when the sample moved by the size of one pixel. Thus, every part of the specimen was imaged for a certain number of times after moving from the first line to the last. For example, N lines of detector were used to image the central strip of the sample in Fig. 1(b). In this case, the width of the red dot box was equal to one pixel. The sample was moved from right to left. N different images were captured for complete imaging of the red dot box. The red dot box was detected by line 1 and line 2 detectors at times t1 and t2, respectively. The time interval was equal to the exposure time of sCMOS. Similar to the red dot box, each part of the sample was detected N times when the sample was moved from line 1 to line N. After imaging the sample, N frames were obtained and corresponding line images (first line image from the first frame, the second line image from the second frame, until the Nth line image from the N

#235822 - $15.00 USD Received 11 Mar 2015; revised 17 Apr 2015; accepted 17 Apr 2015; published 23 Apr 2015

frame) were picked out for signal integration. The data processing algorithm was written in Matlab and the final image was reconstructed on a workstation (Precision T5610, Dell).

The strategy of imaging large tissues is shown in Fig. 1(c). A large rectangle shown in red dots represents the scanning area. As the specimen is moved into the field of interest (i.e., the area between A and B) along the X axis, a signal is generated from the motion stage, which triggers continuous and automatic sCMOS imaging. The imaging length can be adjusted by setting the frame number of sCMOS. The motion stage moves by a strip width, Δy, along the Y axis after complete imaging of one strip. So samples require several image strips to cover entire sample area.

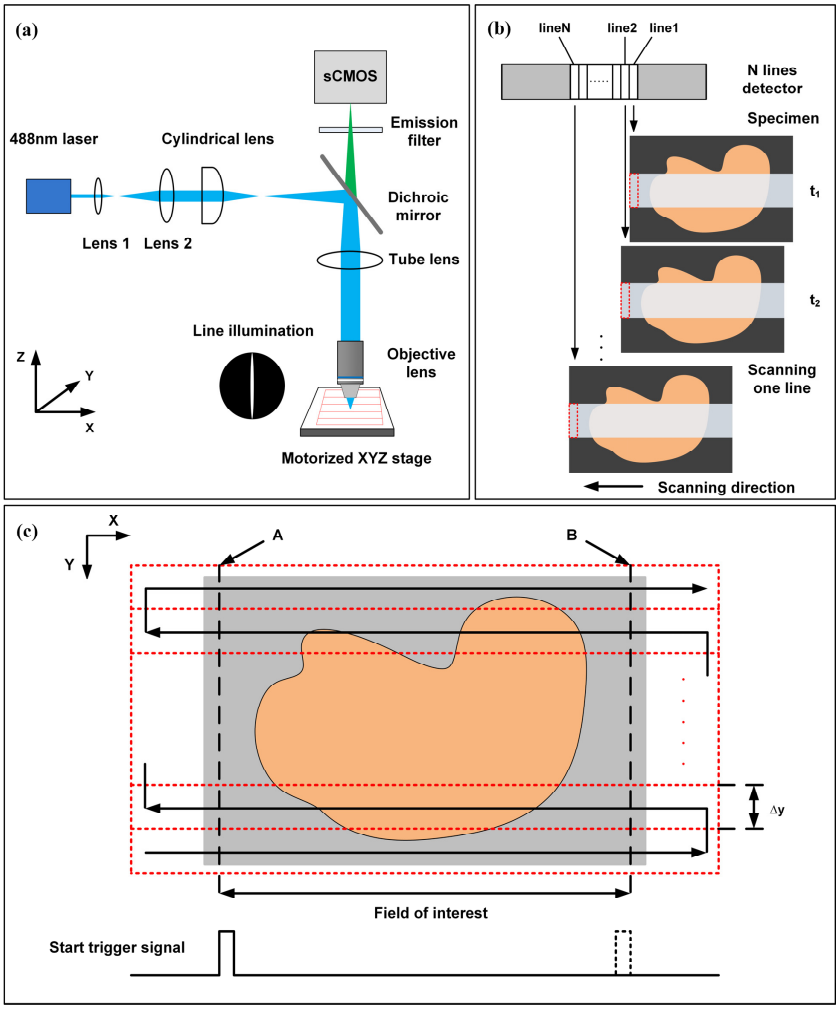

Fig. 1. (a) Schematic configuration of the stage-scanning microscope. A diffraction-limited illumination line was provided on the sample by an optical system. (b) Schematic representation of the method for specimen imaging. (c) Schematic representation of the strategy of large tissue imaging.

3. Results and discussion

3.1 SNR using different number of line detectors

Conventional line scanning confocal microscopy changes slit width in front of the linear detector for rejecting out-of-focus light. In our system, the working mode of sCMOS functions as a physical slit to capture confocal images which only a few lines at the center position are

#235822 - $15.00 USD Received 11 Mar 2015; revised 17 Apr 2015; accepted 17 Apr 2015; published 23 Apr 2015

used to capture the signal. Optimum contrast for different objective and different imaging requirements can be achieved by adjusting the number of line detectors. Figure 2 shows observed SNR by using different line numbers. The sCMOS was set in the sub-array mode that only 8 lines in the center can capture the signal. And 1, 2, 4, 6, and 8 lines were chosen by the software for imaging fluorescent beads. The signal-noise-ratio (SNR) was calculated using the following equation: $SNR = I_{sig} / \sigma_{bkg}$; where I_{sig} is the signal amplitude of single fluorescent beads, and σ_{bkg} is the standard deviation of background around fluorescent beads. The signal increased rapidly as line numbers increased, and decreased rapidly when the total line width was larger than the emission line width. The highest SNR was achieved when 4 lines in the center were used for imaging. One airy unit (AU) can be calculated using equation: $1\ AU = 1.22\lambda/NA$, where λ is wavelength of laser. For a 40 × 0.8 NA objective lens and 488nm laser, 1 AU is 0.74 μm. Width of 4 lines is 0.88 AU.

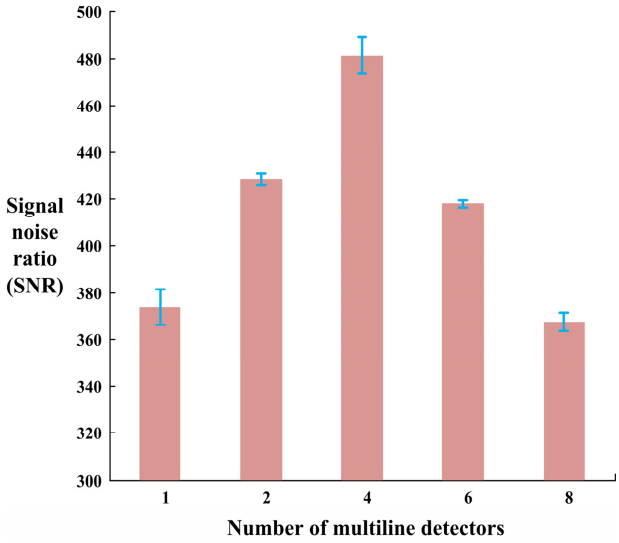

Fig. 2. Signal to noise ratios obtained using varying number of line detectors. A 40 × , 0.8 NA water objective lens was used. Widths of 1, 2, 4, 6, and 8 lines correspond to 0.22, 0.44, 0.88, 1.32, and 1.76 AU. Data represent the mean ± standard deviation of results obtained in 5 different fluorescent beads.

3.2 Measurement of lateral and axial point spread function

Spatial resolution of the system under a 40 × 0.8 NA water objective lens is shown in Fig. 3. Fluorescent beads (200 nm) were used to measure the point spread function (PSF) of optical system by using 4 detection lines. Gaussian fits for X, Y, and axial PSF are shown in red, blue, and green lines, respectively. In Fig. 3(a), FWHM in X and Y direction were 0.47 μm ± 0.02 μm (n = 5) and 0.56 μm ± 0.01 μm (n = 5), respectively. The resolution in the X direction was slightly better than in the Y direction because line illumination was focused along the X direction [18]. Axial resolution was measured by monitoring the signal after moving one mirror from an out-of-focus plane to a focus plane along the z direction by using a step size of 500 nm. In Fig. 3(b), the axial FWHM is 1.56 μm ± 0.05 μm (n = 5).

#235822 - $15.00 USD Received 11 Mar 2015; revised 17 Apr 2015; accepted 17 Apr 2015; published 23 Apr 2015

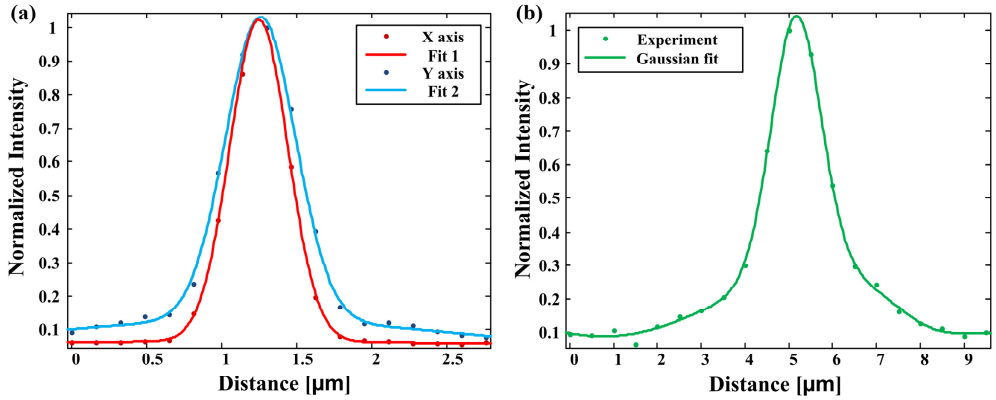

Fig. 3. Measurement of the lateral and axial point spread function. (a) Lateral normalized intensity distribution of fluorescent beads. Red line represents Gaussian fit in X direction and blue line represents Gaussian fit in Y direction. The FWHM in X and Y directions are 0.47 μm ± 0.02 μm and 0.56 μm ± 0.01 μm(n = 5), respectively. (b) Axial normalized intensity distribution of fluorescent beads. Green line represents Gaussian fit. The FWHM in Z direction is 1.56 μm ± 0.05 μm (n = 5).

3.3 Confocal imaging of biological sample

Thy1-enhanced green fluorescent protein (Thy1-EGFP) transgenic mouse and Thy1-enhanced yellow fluorescent protein (Thy1-EYFP) transgenic mouse were chosen as the experiment samples. They were anesthetized with ketamine and perfused transcardially with 0.01M phosphate-buffered saline (PBS) and 4% paraformaldehyde (PFA). After overnight postfixing of the dissected brains at 4°C in 4% PFA, the coronal slices were obtained by sectioning the brains with vibratome (Leica VT1000 S).

A 50-μm-thick Thy1-EYFP transgenic mouse brain slice was used to demonstrate the background rejection performance of this system. A 4-line detector was used to image the brain slice [Fig. 4(a)]. The high contrast of the image was sufficient to visualize the morphological details of neurons, such as dendrite spines. Figure 4(b) shows the result of a wide-field image wherein the structural details are obscured. These results demonstrate the ability of our system to reject the background signal to achieve better image contrast. Figure 4(c) shows the normalized intensity curve along the line in Figs. 4(a) and 4(b). The curve illustrates that the mouse brain slice has better image contrast when imaged in our system.

#235822 - $15.00 USD Received 11 Mar 2015; revised 17 Apr 2015; accepted 17 Apr 2015; published 23 Apr 2015

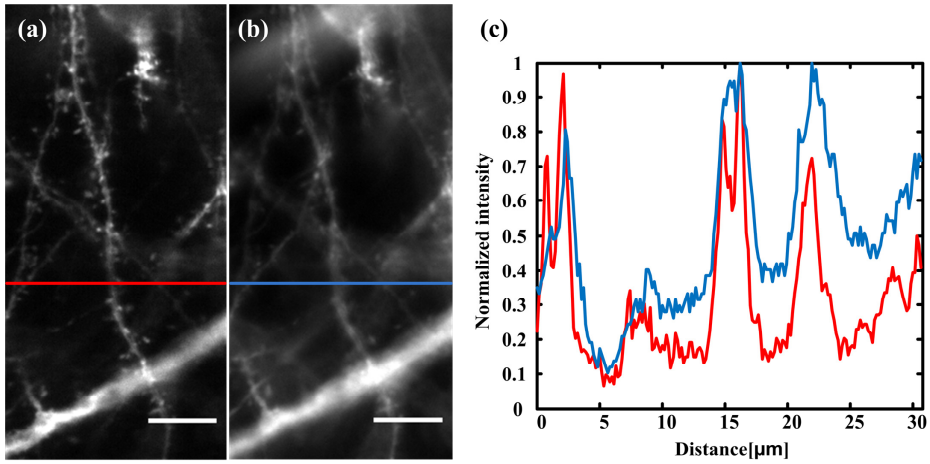

Fig. 4. Imaging of a 50-μm-thick brain slice. (a) Image recorded using the stage-scanning confocal system. The visual slit width is 4 lines. (b) Image recorded using the wide-field image system. (c) The normalized intensity curve along the line in (a) and (b). Scale bar, 10 μm.

A 70-μm-thick Thy1-EGFP transgenic mouse brain slice was imaged in three dimensions with 4-line detector. Z-stack with 30 images was acquired with 1.5μm as a step size. Figure 5 shows the maximum intensity projection result of 45μm z-stack. Two image regions were enlarged which are marked as red box. Because the imaging system provides good optical sectioning, the dendrite spines and axon fibers can be easily identified from the imaging result.

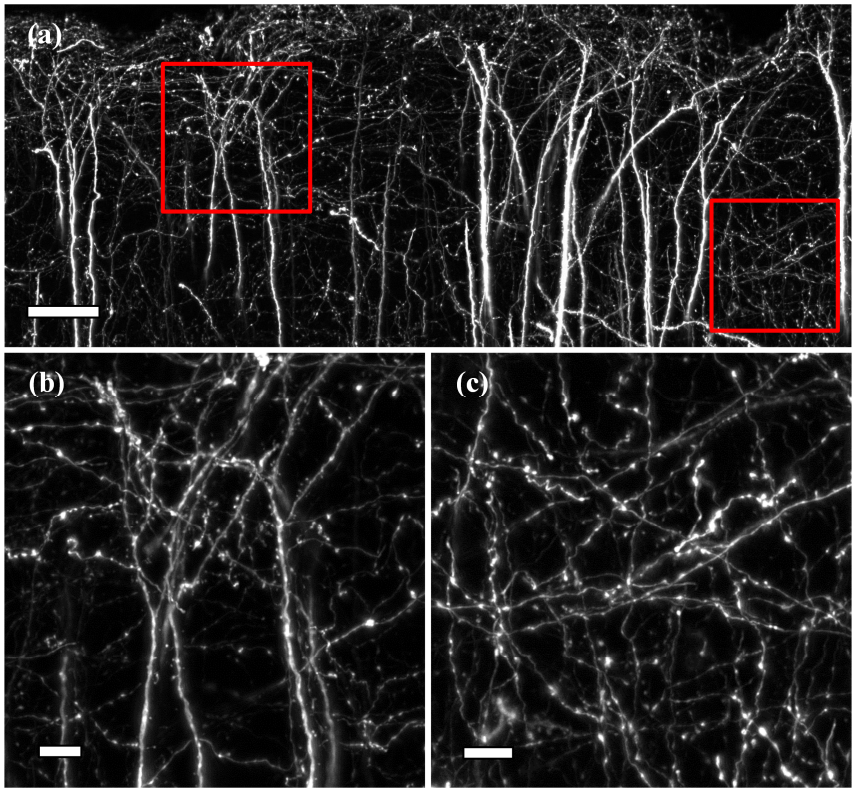

Fig. 5. (a) Maximum intensity projection of 45μm z-stack. Scale bar: 50μm. (b) (c) Enlarged images which were marked as red box in (a). Scale bar: 10μm.

#235822 - $15.00 USD Received 11 Mar 2015; revised 17 Apr 2015; accepted 17 Apr 2015; published 23 Apr 2015

3.4 Imaging of a large area sample

Figure 6 shows results of imaging of a 20-μm-thick Thy1-enhanced green fluorescent protein (Thy1-EGFP) transgenic mouse brain slice. The region imaged in Fig. 6(a) had following dimensions: width, 1.628 mm; and length, 3.328 mm. The sampling resolution was 0.16 μm/pixel. The exposure time was increased to obtain a stronger signal since the fluorescent signal of the brain slice was very weak. The motion speed was set to 61 mm/min and about 20 s were required to image the whole region. The imaging time can be reduced using an excitation laser with higher power or when the signal from the sample is stronger. Figures 6(b)-6(e) show enlarged views of the red box shown in Fig. 6(a). Neuronal fibers can be easily distinguished. Dendritic spines, boutons, and axons can also be seen in the whole imaging regions.

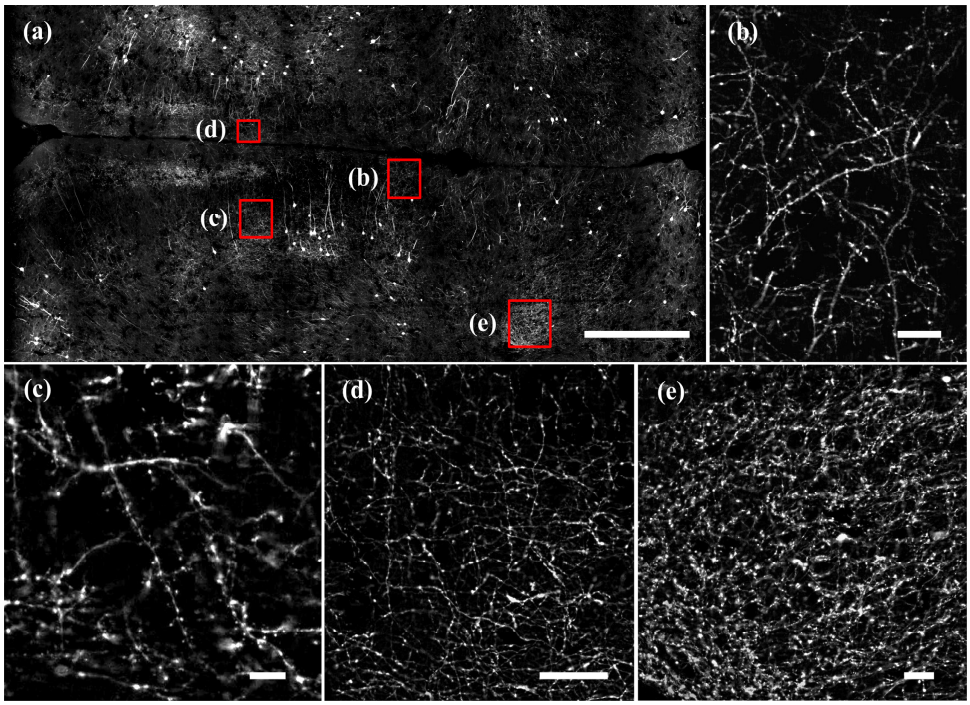

Fig. 6. Imaging of a large area mouse brain slice. (a) The imaged region is about 1.628 mm wide and 3.328 mm long. Scale bar: 500 μm. (b) (c) (d) (e) Enlarged images of brain regions marked as red box in (a). The enlarged images demonstrate visualization of dendrites spine, buttons, and axon fibers in the whole imaging regions. Scale bar, 20 μm.

4. Conclusion

Here, we describe a stage-scanning line confocal microscopy for detail visualization of large tissues. The imaging system uses line scanning methods and strip imaging strategy to increase the imaging speed. The scientific CMOS was used as line detector in sub-array mode and users can adjust the optical sectioning ability by changing the number of line detector according to difference samples. It will be a powerful tool in mouse brain neuron structure imaging. Recent years, there are several imaging systems which can image the whole mouse brain neuron network. However, they all suffered from the balance of high-resolution and high speed. Serial two-photon tomography (STP) [19] and fluorescence micro-optical sectioning tomography (fMOST), two-photon fluorescence micro-optical sectioning tomography (2p-fMOST) achieves high-resolution fluorescence imaging of mouse brain, but the imaging time of one coronal plane is 335sec with sampling resolution of 0.5μm × 0.5μm, 134sec with sampling resolution of 1.0μm × 0.8μm and 124sec with sampling resolution of 0.5μm × 0.5μm,

#235822 - $15.00 USD Received 11 Mar 2015; revised 17 Apr 2015; accepted 17 Apr 2015; published 23 Apr 2015

respectively, which is too slowly for neural research. Stage-scanning line confocal microscopy can image one 10 × 10 mm^2 coronal plane with high sampling resolution of 0.16μm × 0.16μm in about 88sec with maximum speed. An additional advantage of our system is the ease of adjusting the sampling rate. In cases where 1 μm/pixel sampling resolution is enough to visualize biological structures, 6 lines in our system can be combined together to image the tissues which can achieve a high motion speed of 25 mm/s and a 10 × 10 mm^2 coronal plane could be only imaged in about 27 sec. This can be very useful in studying inflammation of mouse colon or detecting the cancer margins rapidly in surgical oncology.

Acknowledgments

We thank X. Liu, Z. Zhou, and Q. Hu of Britton Chance Center for Biomedical Photonics for advices. This work is supported by the National Major Scientific Research Program of China (No. 2011CB910401), the National Nature Science Foundation of China (Grant Nos. 81127002, 30925013, 91232306), Science Fund for Creative Research Group of China (Grant No. 61121004) and 985 project.

#235822 - $15.00 USD Received 11 Mar 2015; revised 17 Apr 2015; accepted 17 Apr 2015; published 23 Apr 2015